Li *et al. J Cancer Metastasis Treat.* 2025;11:1
DOI: 10.20517/2394-4722.2024.77

Journal of Cancer Metastasis and Treatment

Original Article

Open Access

Knockdown of the *EEF1A2* gene reduces lung cancer brain metastasis by downregulating the *BCL10/NFκB* pathway

Bo Li[1], Jinyi Zhou[1], Kai Ding[2], Songyu Liu[3], Lu Zhang[3], Bin Zeng[2], Hongping Yuan[1], Pin Zuo[1], Chun Wang[4], Shujuan Li[4], Jun Wang[2], Yaodong Fan[1], Xiaosan Su[5]

[1]Department of Neurosurgery, The Third Affiliated Hospital of Kunming Medical University, Kunming 650118, Yunnan, China.
[2]Department of Anesthesiology, The First Affiliated Hospital of Kunming Medical University, Kunming 650032, Yunnan, China.
[3]School of Basic Medical Sciences, Yunnan University of Chinese Medicine, Kunming 650500, Yunnan, China.
[4]Department of PET-CT/MR Center, The Third Affiliated Hospital of Kunming Medical University, Kunming 650118, Yunnan, China.
[5]Scientific Research and Experimental Center, Yunnan University of Chinese Medicine, Kunming 650500, Yunnan, China.

Correspondence to: Dr. Xiaosan Su, Scientific Research and Experimental Center, Yunnan University of Chinese Medicine, 1076 Yuhua Road, Chenggong District, Kunming 650500, Yunnan, China. E-mail: suxs163@163.com; Dr. Yaodong Fan, Department of Neurosurgery, The Third Affiliated Hospital of Kunming Medical University, No. 519 Kunzhou Road, Xishan District, Kunming 650118, Yunnan, China. E-mail: fyd5188@aliyun.com

How to cite this article: Li B, Zhou J, Ding K, Liu S, Zhang L, Zeng B, Yuan H, Zuo P, Wang C, Li S, Wang J, Fan Y, Su X. Knockdown of the *EEF1A2* gene reduces lung cancer brain metastasis by downregulating the *BCL10/NFκB* pathway. *J Cancer Metastasis Treat.* 2025;11:1. https://dx.doi.org/10.20517/2394-4722.2024.77

Received: 27 Jul 2024 **First Decision:** 8 Oct 2024 **Revised:** 15 Dec 2024 **Accepted:** 2 Jan 2025 **Published:** 16 Jan 2025

Academic Editor: Ciro Isidoro **Copy Editor:** Fangling Lan **Production Editor:** Fangling Lan

Abstract

Aim: Brain metastases (BM) in patients with lung cancer (LC) are linked to unfavorable outcomes. The eukaryotic translation elongation factor 1 alpha 2 (EEF1A2) is notably overexpressed across various cancer types and plays a role in promoting tumor initiation and progression. This research aimed to clarify the function of EEF1A2 in the context of lung cancer brain metastasis (LCBM) and to explore the mechanisms underlying its effects.

Methods: To identify genes with differential expression between LC and LCBM samples, transcriptomic microarray analyses were conducted, confirming that EEF1A2 expression is elevated in LCBM. EEF1A2 expression levels were validated in multiple LC cell lines. PC9 and SPCA1 cells were transfected with lentiviral vectors carrying siRNAs targeting EEF1A2 to assess its role both *in vitro* and *in vivo*. Tandem mass tag proteomics was employed to identify proteins regulated by EEF1A2. The expression of EEF1A2, BCL10, and phosphorylated NF-κB in tumor tissues from LC and LCBM patients was analyzed.

Results: Compared to the LC samples, the LCBM samples exhibited significantly higher levels of EEF1A2 expression. EEF1A2 knockdown in PC9 and SPCA1 cells resulted in substantial reductions in cell proliferation, migration, and invasion. Proteomic profiling revealed that BCL10 protein levels were markedly reduced in EEF1A2-knockdown cells. Additionally, there was a decrease in phosphorylated NF-κB, EGFR, and mesenchymal markers (N-cadherin, Twist, Snail, Slug, and Cdc42), along with an increase in E-cadherin expression. In a mouse model, EEF1A2 knockdown in PC9 cells significantly inhibited brain metastasis. Furthermore, patient samples presented elevated levels of EEF1A2, BCL10, and phosphorylated NF-κB in LCBM tissues than in LC tissues.

Conclusion: Our research revealed that EEF1A2 is upregulated in LCBM, and that its knockdown suppresses brain metastasis by decreasing BCL10 expression, inhibiting NF-κB signaling, and reducing epithelial-mesenchymal transition markers. These results suggest that targeting EEF1A2 may be a promising therapeutic approach for preventing and treating brain metastasis in lung cancer patients.

Keywords: Eukaryotic translation elongation factor 1 alpha 2 (EEF1A2), lung cancer brain metastasis, BCL10, NFκB, epithelial-mesenchymal transition (EMT)

INTRODUCTION

Lung cancer remains among the most widespread and deadly malignancies, responsible for around 1.79 million deaths globally each year[1]. Approximately 50% of non-small cell lung cancer (NSCLC) patients develop brain metastases, significantly worsening prognosis and reducing median survival to three months[2]. Existing treatments for lung cancer brain metastasis (LCBM) - including surgery, radiation therapy, chemotherapy, immunotherapy, and targeted therapies - often yield unsatisfactory results. This highlights the urgent need to deepen our understanding of the biological and molecular mechanisms driving this aggressive disease and to identify new therapeutic targets[3].

Eukaryotic translation elongation factor 1 alpha 2 (EEF1A2) is a crucial member of the conserved EEF1A family of GTP-binding enzymes that are essential for protein synthesis in eukaryotic cells[4]. Its canonical role involves delivering aminoacyl-tRNA to the ribosomal A site during the elongation phase of protein synthesis[5]. However, EEF1A2 has garnered significant interest in oncology because of its overexpression in various malignancies - including ovarian, breast, lung, and liver cancers - positioning it as a putative oncogene[6-10]. Research has linked EEF1A2 to tumor development and metastasis, with studies reporting its role in enhancing the invasive capabilities of breast cancer cells and facilitating pancreatic cancer metastasis[11,12]. Mechanistically, EEF1A2 stimulates cancer cell proliferation, migration, and invasion via activation of the PI3K/AKT signaling pathway and induction of epithelial-mesenchymal transition (EMT). Moreover, silencing EEF1A2 expression can attenuate cell proliferation and induce cell cycle arrest[13,14]. However, its specific contributions to the LCBM remain unknown.

In this study, we employed whole-transcriptome microarray analysis to profile LC and LCBM samples and identify DEGs. Through *in vitro* and *in vivo* studies, we established that EEF1A2 is directly associated with the proliferation, invasion, and migration of LC cells. The mechanisms underlying these EEF1A2-associated effects were investigated in EEF1A2-knockdown LC cells. These results establish a foundation for developing novel therapeutic strategies that target EEF1A2 in LCBM.

METHODS

Sample collection and preparation

From April 2019 to October 2021, we obtained five matched pairs of LC and LCBM samples from patients undergoing surgical procedures at the Third Affiliated Hospital of Kunming Medical University. To ensure

their integrity for future analyses, the excised samples were immediately preserved in liquid nitrogen. Prior to their inclusion in the study, histopathological examinations confirmed each sample as adenocarcinoma. Informed consent was secured from all participants before collecting and utilizing their biological samples. This research was approved by the Ethics Committee of the Third Affiliated Hospital of Kunming Medical University.

Human ceRNA microarray detection and analysis

For transcriptome analysis, we used the Agilent Human ceRNA Microarray 2019 (4 × 180 K, Design ID: 086188). Total RNA extracted from the ten samples was quantified with a NanoDrop ND-2000 spectrophotometer (Thermo Fisher Scientific, Waltham, MA, USA), and RNA integrity was evaluated using an Agilent Bioanalyzer 2100 (Agilent Technologies, Santa Clara, CA, USA). This RNA was utilized for sample labeling, microarray hybridization, and washing procedures. Briefly, double-stranded RNA was reverse-transcribed into cDNA, which was then transcribed into complementary RNA (cRNA) and labeled with cyanine-3-CTP. Following hybridization and washing, the microarrays were scanned using an Agilent G2505C scanner. Raw data were extracted from the array images using Feature Extraction software (version 10.7.1.1; Agilent Technologies) and normalized through a quantile algorithm. Probes identified as "detected" under either condition were selected for further analysis. Differentially expressed genes (DEGs) were determined based on a fold change of $|FC| \geq 2.0$ and statistical significance ($P < 0.05$) calculated from *t*-tests. Data analysis for all samples was performed by OE Biotechnology Co., Ltd. (Shanghai, China).

GO and KEGG analysis

Our results were derived from functional enrichment analyses of long noncoding RNAs (lncRNAs) and their target mRNAs via OECloud (http://cloud.oebiotech.cn). We performed analyses using the Gene Ontology (GO) and Kyoto Encyclopedia of Genes and Genomes (KEGG) pathways. The significance of gene enrichment was assessed by employing hypergeometric distribution algorithms.

LncRNA-miRNA-mRNA network construction

We calculated Pearson correlation coefficients to evaluate relationships among RNA species. Differentially expressed lncRNAs that were positively coexpressed with differentially expressed mRNAs were selected for ceRNA analysis. Known miRNAs from the miRBase22 database aided in predicting were used to predict miRNA targets of both lncRNAs and mRNAs. Using miRNAs as bridges, we constructed and visualized a ternary lncRNA-miRNA-mRNA ceRNA network.

Database

We extracted EEF1A2 gene expression profiles from malignant and adjacent normal tissues of lung adenocarcinoma (LUAD) and lung squamous cell carcinoma (LUSC) patients using The Cancer Genome Atlas (TCGA) and Genotype-Tissue Expression (GTEx) databases. These datasets were analyzed utilizing GEPIA2 (http://gepia2.cancer-pku.cn). Kaplan-Meier survival analysis was performed with the Kaplan-Meier plotter tool (https://kmplot.com), which combines data from the GEO, EGA, and TCGA repositories.

Cell culture

Human bronchial epithelial (HBE) cells and lung cancer cell lines - A549, H460, SPCA1, PC9, and 95D - were sourced from the Shanghai Cell Bank of the Chinese Academy of Sciences. The cells were maintained in RPMI 1640 medium supplemented with 10% fetal bovine serum (FBS; VivaCell, Shanghai, China) under humidified conditions at 37 °C with 5% CO_2.

Establishment of transfected lung cancer cell lines

Lentiviruses encoding EEF1A2 shRNA or negative control sequences - both constructs carrying genes for green fluorescent protein (GFP) and puromycin resistance - were constructed by GenePharma (Shanghai, China; see Supplementary Materials for details). Viral titers were assessed through serial dilution. PC9 and SPCA1 cells were infected with lentiviruses at a concentration of 9×10^8 TU/mL in the presence of 2 μg/mL polybrene. Following a 24-h incubation at 37 °C with 5% CO_2, the medium was replaced, and cells were cultured for an additional 48 h. Stable cell lines were generated by selecting with 1 μg/mL puromycin over three passages. These cell lines were subsequently used in further experiments.

Reverse transcription-quantitative polymerase chain reaction (RT-qPCR) analysis

Total RNA was isolated from lung cancer cells or clinical samples using TRIzol reagent (Invitrogen, MA, USA) according to the manufacturer's protocol, and reverse-transcribed into complementary DNA (cDNA) with the PrimeScript RT Kit (Takara, Beijing, China). PCR amplification was conducted using the SYBR Green RT-PCR kit (Takara) on a StepOne Plus real-time PCR system (Thermo Fisher Scientific, MA, USA), employing GAPDH as an internal control. Data analysis was performed using the $2^{-\Delta\Delta CT}$ method. The primer sequences used were as follows: EEF1A2 forward, 5′-GTCAAGGAAGTCAGCGCCTA-3′, reverse, 5′-CCTAATCCAGCTTCTTGCGAAC-3′; GAPDH forward, 5′-AGATCCCTCCAAAATCAAGTGG-3′, reverse, 5′-GGCAGAGATGATGACCCTTTT-3′.

Western blotting

Cells were lysed using RIPA buffer (Proteintech, Wuhan, China) supplemented with protease and phosphatase inhibitors like PMSF. Protein concentrations were measured using the bicinchoninic acid (BCA) assay. Lysates containing 30-50 μg of protein were separated by SDS-PAGE and transferred onto PVDF membranes. The membranes were then incubated with primary antibodies against EEF1A2 (#ab227824, Abcam), BCL10 (#50180-1-AP, Proteintech), NFκB (#250060, ZenBio Science), phosphorylated NFκB (#310012, ZenBio Science), EGFR (#18986-1-AP, Proteintech), phosphorylated EGFR (#ab40815, Abcam), GAPDH (#10494-1-AP, Proteintech), Cyclin D1 (#26939-1-AP, Proteintech), p21 (#381102, ZenBio Science), Snail/Slug (#ab180714, Abcam), N-cadherin (#ab76011, Abcam), E-cadherin (#ab76055, Abcam), Twist (#ab175430, Abcam), and Cdc42 (#10155-1-AP, Proteintech). Following incubation with secondary antibodies, target proteins were visualized via enhanced chemiluminescence detection reagents (Proteintech) and a multifunctional gel imaging system.

Cell counting kit-8 assay

Cell proliferation was evaluated using the Cell Counting Kit-8 (CCK-8; Proteintech) per the manufacturer's instructions. Briefly, SPCA1 and PC9 cells with EEF1A2 knockdown and their control counterparts were seeded into 96-well plates at a density of 5×10^3 cells per well in 100 μL of complete medium. Cells were cultured at 37 °C in a humidified incubator with 5% CO_2. At specific time points (24, 48, 72, and 96 h), 10 μL of CCK-8 solution was added to each well, followed by an additional 2 h of incubation under the same conditions. Absorbance was measured at 450 nm using a Bio-Rad microplate reader. Each assay was conducted in triplicate, and experiments were independently repeated three times.

Wound healing assay

EEF1A2-knockdown SPCA1 and PC9 cells, along with control cells, were seeded into 6-well plates at 1×10^5 cells per well and cultured until they reached approximately 80% confluence. The culture medium was removed, and the cell monolayers were gently rinsed twice with phosphate-buffered saline (PBS) to eliminate residual medium and non-adherent cells. Uniform linear scratches ("wounds") were made across the monolayers using a sterile 200 μL pipette tip. After scratching, wells were washed again with PBS to remove detached cells. Cells were then incubated in serum-free medium to minimize proliferation and

assess migration. At 0 and 24 h post-scratch, images of the wound areas were captured using an inverted microscope. Wound closure was quantified by measuring the wound area at each time point with ImageJ software, calculating the percentage of closure relative to the initial wound size. Experiments were performed in triplicate and repeated independently three times to ensure reproducibility and reliability.

Transwell migration and invasion assays

For the migration assay, 50,000 cells in 200 μL of serum-free medium were placed in the upper chamber of a transwell insert (NEST, Wuxi, China). For the invasion assay, the upper chamber was coated with Matrigel. The lower chamber contained 600 μL of medium with 10% FBS as a chemoattractant. After 24 h, cells remaining in the upper chamber were removed. Migrated cells on the lower membrane surface were fixed, stained with crystal violet, and observed under an inverted microscope. Cell numbers were quantified using ImageJ software. All assays were performed in triplicate.

In vivo model of lung cancer brain metastasis

In this study, groups of ten four-week-old female BALB/c nude mice were used, sourced from Slake Jingda Laboratory in Hunan, China. Each mouse was injected with 1×10^5 tumor cells suspended in 0.1 mL PBS into the common carotid artery. The mice were euthanized on day 50 postinoculation or earlier if they displayed clinical signs of brain metastases, such as immobility, weight loss, or hunching. After the animals were euthanized, brain tissues were harvested, sliced into 4-μm sections, and stained with hematoxylin and eosin (H&E) for histopathological examination. This research was approved by the Animal Experimentation Ethics Committee of the Third Affiliated Hospital of Kunming Medical University.

Immunohistochemical analysis

The tissue sections were deparaffinized in xylene and rehydrated through a graded ethanol series. Antigen unmasking was achieved using citrate buffer, and intrinsic peroxidase activity was inhibited with hydrogen peroxide (H_2O_2). The sections were blocked with rabbit or goat serum to prevent nonspecific binding. Primary antibodies against EEF1A2, BCL10, and phosphorylated NFκB were applied, followed by enzyme-labeled secondary antibodies. Proteins were visualized with diaminobenzidine and counterstained with hematoxylin to enhance contrast.

Lung cancer and lung cancer brain metastasis samples

From September 2020 to August 2023, a study at The Third Affiliated Hospital of Kunming Medical University included 21 patients with LC and 21 with LCBM. The research was approved by the hospital's ethics committee, and all participants provided written informed consent for the use and publication of their anonymized medical information. Samples were preserved in liquid nitrogen, and clinical data are detailed in Table 1.

Statistical analysis

Statistical analyses were conducted using GraphPad Prism v8.0 (GraphPad Software, La Jolla, CA, USA). One-way ANOVA was applied for comparisons among multiple groups. For comparisons between two groups, either Student's *t*-test or the Mann-Whitney *U* test was utilized, depending on the data distribution. Results are expressed as means ± standard deviations (SDs). A *P*-value less than 0.05 was considered statistically significant.

RESULTS

Variations in the expression profiles of lncRNAs and mRNAs between LCBM and LC

To identify lncRNAs and mRNAs implicated in LCBM, we analyzed five matched pairs of LCBM and LC samples via a competing endogenous RNA (ceRNA) microarray. Among the 100,831 lncRNAs detected,

Table 1. Clinical information of LC and LCBM patients

Factor	LC (n = 21)	LCBM (n = 21)	P value
Gender			0.087[1]
Male	8	14	
Female	12	7	
Age			0.489[2]
≥ 65	7	5	
< 65	11	15	
Histology			0.086[2]
Ad	15	12	
Sq	/	3	
Un	1	5	
Tumor markers			
CEA (ng/mL)			0.626[2]
≥ 25	1	4	
< 25	10	15	
CA125 (kU/L)			1[2]
≥ 35	2	5	
< 35	9	14	
CA153 (U/mL)			1[1]
≥ 28	1	3	
< 28	10	15	
CA242 (U/mL)			1[2]
≥ 20	/	3	
< 20	5	16	
CA724 (U/mL)			1[2]
≥ 6.9	2	6	
< 6.9	3	12	
CA199 (U/mL)			1[2]
≥ 37	1	2	
< 37	8	16	
NSE (ng/mL)			0.372[2]
≥ 16.3	1	5	
< 16.3	10	14	

LC: Lung cancer; LCBM: lung cancer brain metastasis, ad: adenocarcinoma, Sq: squamous cell carcinoma, Un: undetermined; [1]Chi-square test; [2]Fisher's exact test.

4,391 exhibited significant differential expression between the LCBM and LC samples ($|\log_2$ fold change$| > 1$, $P < 0.05$). Specifically, comparing LCBM samples with LC samples, we found that 1,755 lncRNAs were upregulated and 2,636 were downregulated [Figure 1A]. Similarly, of the 263,445 mRNAs identified, 2,397 were differentially expressed, with 865 upregulated and 1,532 downregulated in the LCBM samples [Figure 1B]. Figure 1C and D showcase the top 25 upregulated and downregulated lncRNAs and mRNAs, respectively, with EEF1A2 being notably altered among them. When mapping the chromosomal distribution of these differentially expressed mRNAs, it was found that chromosome 7 contained the highest number of upregulated mRNAs (n = 103), followed by chromosome 1 (n = 95) [Figure 1E]. Conversely, chromosome 1 presented the greatest number of downregulated mRNAs (n = 148) [Figure 1F]. These findings suggest that aberrant expression of lncRNAs and mRNAs contributes to the pathogenesis of LCBM.

EEF1A2 is associated with the pathogenesis of LCBM and poor prognosis in lung cancer patients

To identify key genes involved in LCBM formation, we conducted GO and KEGG enrichment analyses. The GO analysis indicated that the upregulated mRNAs in LCBM were significantly enriched in biological processes such as cellular amino acid biosynthesis, aminoacyl-tRNA synthetase multienzyme complexes, and protein transporter activity [Figure 2A]. Conversely, downregulated mRNAs were associated with negative regulation of cell migration, cell adhesion, and focal adhesion [Figure 2B]. KEGG analysis indicated that the upregulated mRNAs were significantly involved in pathways related to the cell cycle and

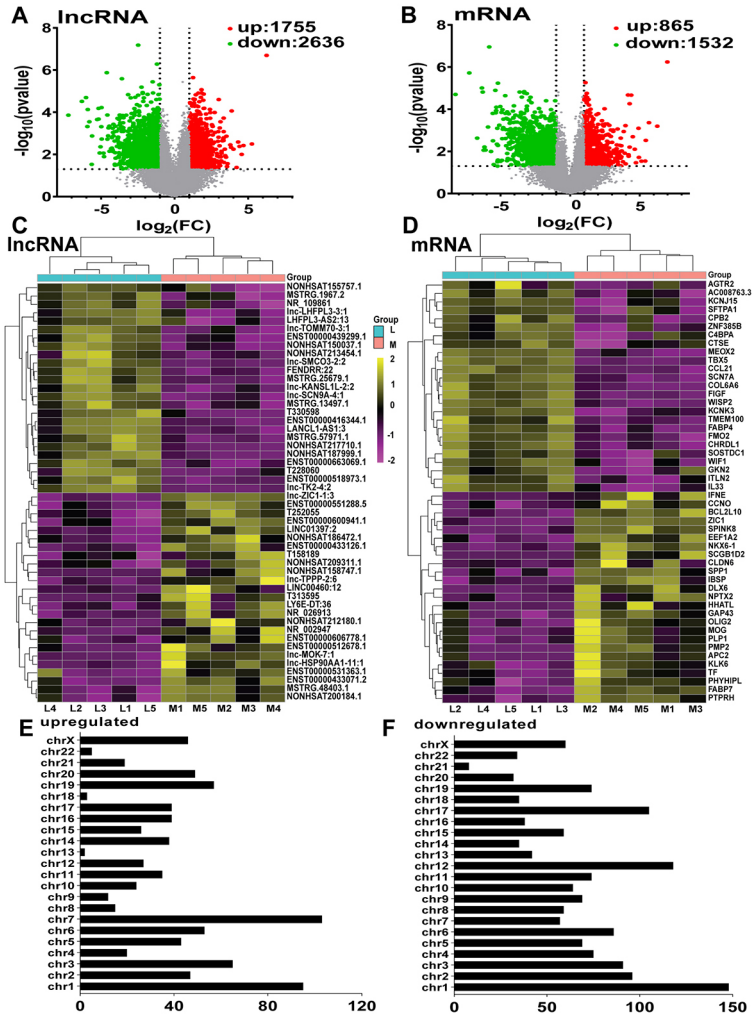

Figure 1. Transcriptomic microarray analysis of lncRNAs and mRNAs in LC and LCBM samples. (A and B) Volcano plots illustrating up- and downregulated lncRNAs and mRNAs in five LCBM samples compared with five other LC samples. (C and D) Heatmaps highlighting the top 25 up- and downregulated lncRNAs and mRNAs. (E and F) Chromosomal distribution of up- and downregulated mRNAs.

purine and pyrimidine metabolism [Figure 2C]. Conversely, the downregulated mRNAs were associated with focal adhesion, extracellular matrix-receptor interactions, and cell adhesion molecules [Figure 2D]. These findings suggest that upregulated genes may promote cell cycle progression and protein synthesis, whereas downregulated genes may contribute to epithelial-mesenchymal transition (EMT), thereby facilitating cancer metastasis.

LncRNAs regulate mRNA transcription, translation, and splicing by competitively binding miRNAs. Employing miRBase v22, we predicted interactions between miRNAs and lncRNAs as well as miRNAs and mRNAs to construct an lncRNA-miRNA-mRNA regulatory network. Comprehensive ceRNA network analysis identified EEF1A2 as a key component [Figure 2E]. We, therefore, examined the role of EEF1A2 in lung cancer development and prognosis. Analysis of TCGA and GTEx data demonstrated that EEF1A2 expression was significantly elevated in LUAD samples compared to adjacent normal tissues ($P < 0.05$; Figure 2F). Furthermore, EEF1A2 expression increased significantly from stages I to IV ($P < 0.05$; Figure 2G). Survival analyses from the GEO and EGA databases indicated that higher EEF1A2 expression is associated with poor prognosis in lung cancer patients (hazard ratio = 1.53, $P < 0.001$; Figure 2H). This finding highlights the significant role of EEF1A2 in the progression of lung cancer and brain metastasis.

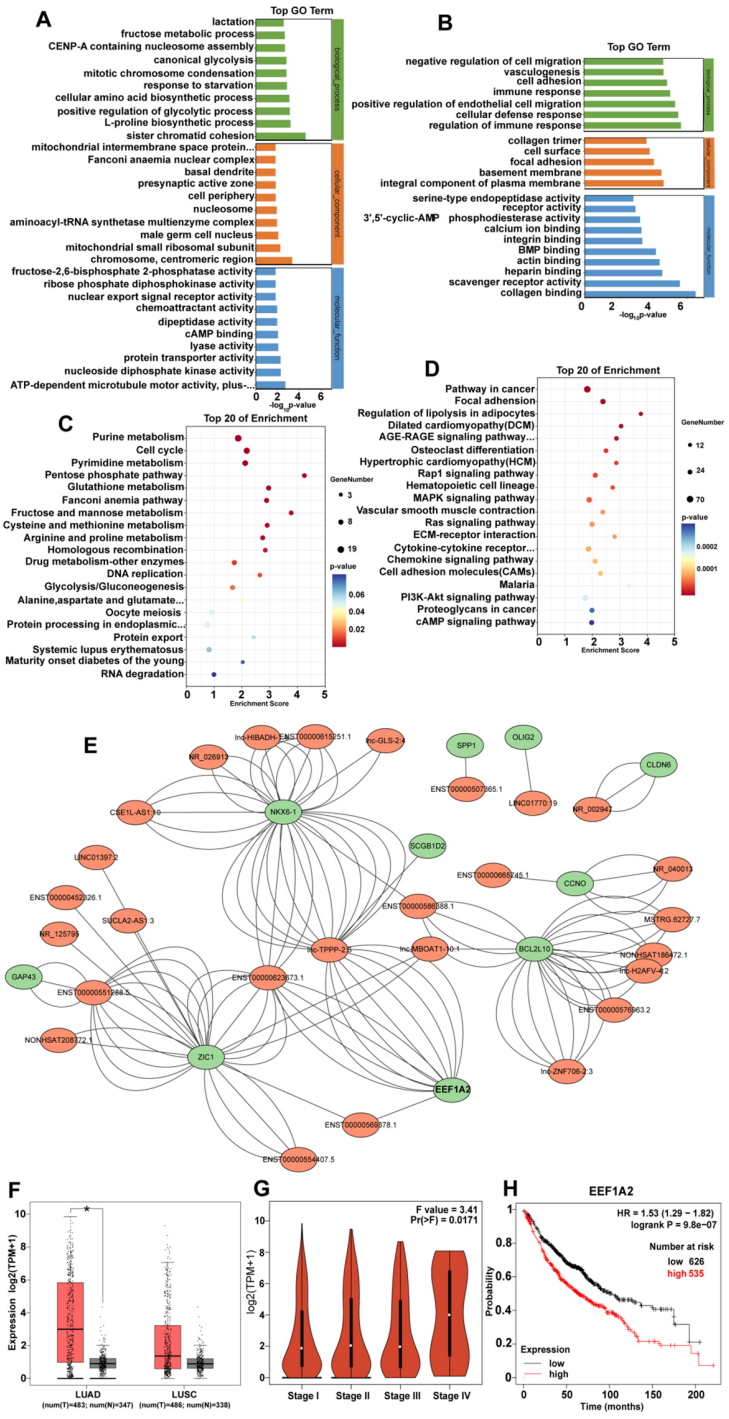

Figure 2. EEF1A2 plays a role in the development of lung cancer brain metastasis (LCBM) and is linked to poor outcomes in lung cancer patients. (A and B) the GO analysis of (A) upregulated and (B) downregulated mRNAs when comparing LCBM to LC groups. (C and D) the KEGG pathway analysis of (C) upregulated and (D) downregulated mRNAs between LCBM and LC groups. (E) CeRNA network incorporating the top 10 upregulated mRNAs. (F) the expression levels of EEF1A2 in tumor tissues (T) *vs.* adjacent normal tissues (N) from LUAD and LUSC patients based on TCGA and GTEx data. (G) EEF1A2 expression across stages I-IV in LUAD and LUSC patients according to TCGA and GTEx datasets. (H) Kaplan-Meier survival curves for overall survival (OS) of LUAD patients with high or low EEF1A2 expression, utilizing data from the TCGA, GEO, and EGA databases. Data are presented as means ± S.D.; $^{*}P < 0.05$.

Silencing EEF1A2 suppresses the in vitro growth, migration, and invasion abilities of lung cancer cells

Analysis of EEF1A2 expression in HBE cells and various lung cancer cell lines revealed significantly elevated levels of EEF1A2 in PC9 and SPCA1 cells [Figure 3A]. To investigate the functional role of EEF1A2, we transduced PC9 and SPCA1 cells with lentiviruses expressing shRNAs targeting EEF1A2, which effectively knocked down EEF1A2, as confirmed by RT-qPCR and Western blot analyses [Figure 3B]. Compared with the control, EEF1A2 knockdown significantly reduced the proliferation of these cells [Figure 3C]. Because the upregulated mRNAs in LCBM were enriched in the cell cycle pathway, we investigated the effects of EEF1A2 silencing on proteins that regulate the cell cycle. Western blot analysis revealed decreased cyclin D1 and increased p21 levels upon EEF1A2 knockdown [Figure 3D]. Furthermore, wound healing and Transwell assays indicated that suppressing EEF1A2 hindered the migration and invasion of PC9 and SPCA1 cells [Figure 3E-G].

Knockdown of EEF1A2 reduces the expression of BCL10, NFκB and EMT-related molecules

To elucidate the mechanisms of EEF1A2, we conducted proteomic analysis on EEF1A2-knockdown PC9 cells and identified 233 upregulated and 295 downregulated proteins, with BCL10 being among the most significantly downregulated [Figure 4A and B]. KEGG pathway analysis revealed that the "apoptosis" pathway was notably affected by EEF1A2 knockdown [Figure 4C]. Western blotting confirmed decreased BCL10 expression in both PC9 and SPCA1 cells lacking EEF1A2 [Figure 4D and E]. Given that BCL10 promotes NFκB activation - a downstream effector of EGFR signaling[15] - we observed reduced levels of phosphorylated EGFR and NFκB in EEF1A2-knockdown cells [Figure 4D and E]. These findings suggest that EEF1A2 influences antiapoptotic mechanisms via the EGFR/BCL10/NFκB axis. Moreover, in PC9 and SPCA1 cells, silencing EEF1A2 led to an increase in E-cadherin expression and a decrease in mesenchymal markers - including N-cadherin, Twist, Cdc42, Snail, and Slug - as shown in Figure 4F and G, indicating that EMT was inhibited. Overall, these findings suggest that EEF1A2 promotes invasion and metastasis in lung cancer cells by facilitating EMT and regulating antiapoptotic signaling pathways.

Knockdown of EEF1A2 suppresses lung cancer brain metastasis in nude mice

To determine the *in vivo* effects of EEF1A2 on lung cancer cell proliferation and metastasis, we developed a brain metastasis model using PC9 cells with EEF1A2 knockdown. The EEF1A2-knockdown group exhibited significant suppression of brain metastasis, as evidenced by reduced tumor size and a lower proportion of lung cancer cells in brain tissues ($P < 0.05$; Figure 5A and B). In addition, immunohistochemical analysis confirmed that brain tumor tissues from the EEF1A2-knockdown group exhibited decreased levels of EEF1A2, BCL10, and phosphorylated NFκB compared to those from the control group [Figure 5C].

Elevated expression of EEF1A2, BCL10, and NFκB in the LCBM

To confirm the association between EEF1A2 and lung cancer brain metastasis LCBM, we conducted RT-qPCR analysis on tumor samples from 21 LC patients and 21 LCBM patients. The results demonstrated significant upregulation of *EEF1A2* gene expression in brain tumor tissues from LCBM patients, accompanied by a concurrent downregulation of E-cadherin gene expression [Figure 6A]. Western blot analysis further revealed elevated protein levels of EEF1A2, BCL10, and phosphorylated NFκB in brain tumor samples from LCBM patients compared with those from LC patients [Figure 6B and C]. These findings suggest that EEF1A2 may promote LCBM through activation of the BCL10/NFκB signaling pathway.

DISCUSSION

Although substantial progress has been made in treating BM, patients with LCBM still suffer from poor prognoses and short survival durations[16]. These findings underscore the urgent need for more effective

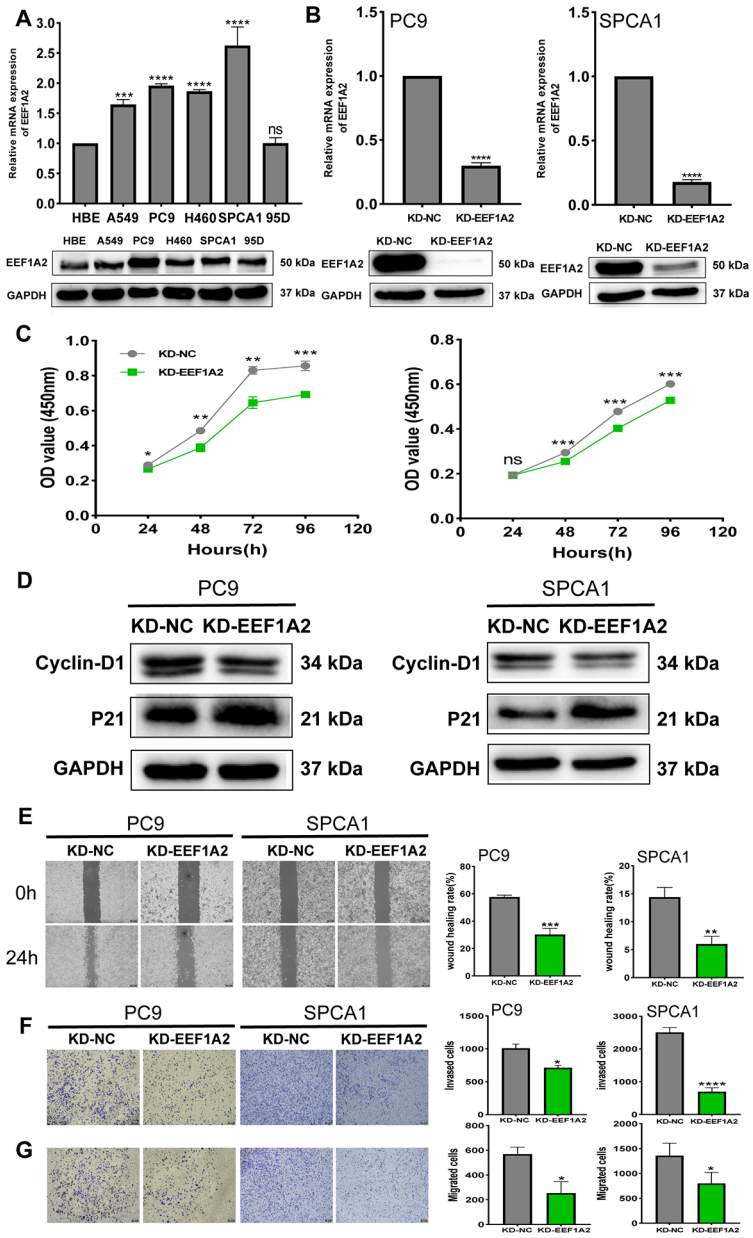

Figure 3. EEF1A2 knockdown suppresses proliferation, migration, and invasion in lung cancer cells. (A) EEF1A2 expression levels in lung cancer cell lines were measured using RT-qPCR and WB analyses. Significance levels are indicated: ***$P < 0.001$, ****$P < 0.0001$; ns denotes no significant difference compared to HBE cells. (B) PC-9 and SPCA1 cells were transfected with shEEF1A2 lentivirus (KD-EEF1A2) or control lentivirus (KD-NC), and EEF1A2 expression was evaluated via RT-qPCR and WB. (C) The proliferation of PC-9 and SPCA1 cells transfected with KD-NC or KD-EEF1A2 was assessed using the CCK-8 assay. Statistical significance is represented as *$P < 0.05$, **$P < 0.01$, ***$P < 0.001$; ns indicates no significant difference compared to the KD-NC group. (D) Western blot analysis was performed to detect cyclin D1 and p21 protein levels in PC-9 and SPCA1 cells after transfection with KD-NC or KD-EEF1A2. (E) Wound healing assays were conducted on PC-9 and SPCA1 cells transfected with KD-NC or KD-EEF1A2 to evaluate their migratory capacity. (F and G) Transwell migration and invasion assays were carried out on PC-9 and SPCA1 cells following transfection with KD-NC or KD-EEF1A2. Statistical significance is indicated by *$P < 0.05$, **$P < 0.01$, ***$P < 0.001$, ****$P < 0.0001$ compared to the KD-NC group.

therapeutic strategies, which may be developed by identifying key genes involved in brain metastasis. Our research identified EEF1A2 as a crucial gene in LCBM, showing significantly higher expression levels compared to primary lung cancer. Experiments conducted *in vitro* showed that silencing EEF1A2 significantly reduced the proliferation, invasion, and migration of lung cancer cells. *In vivo* studies

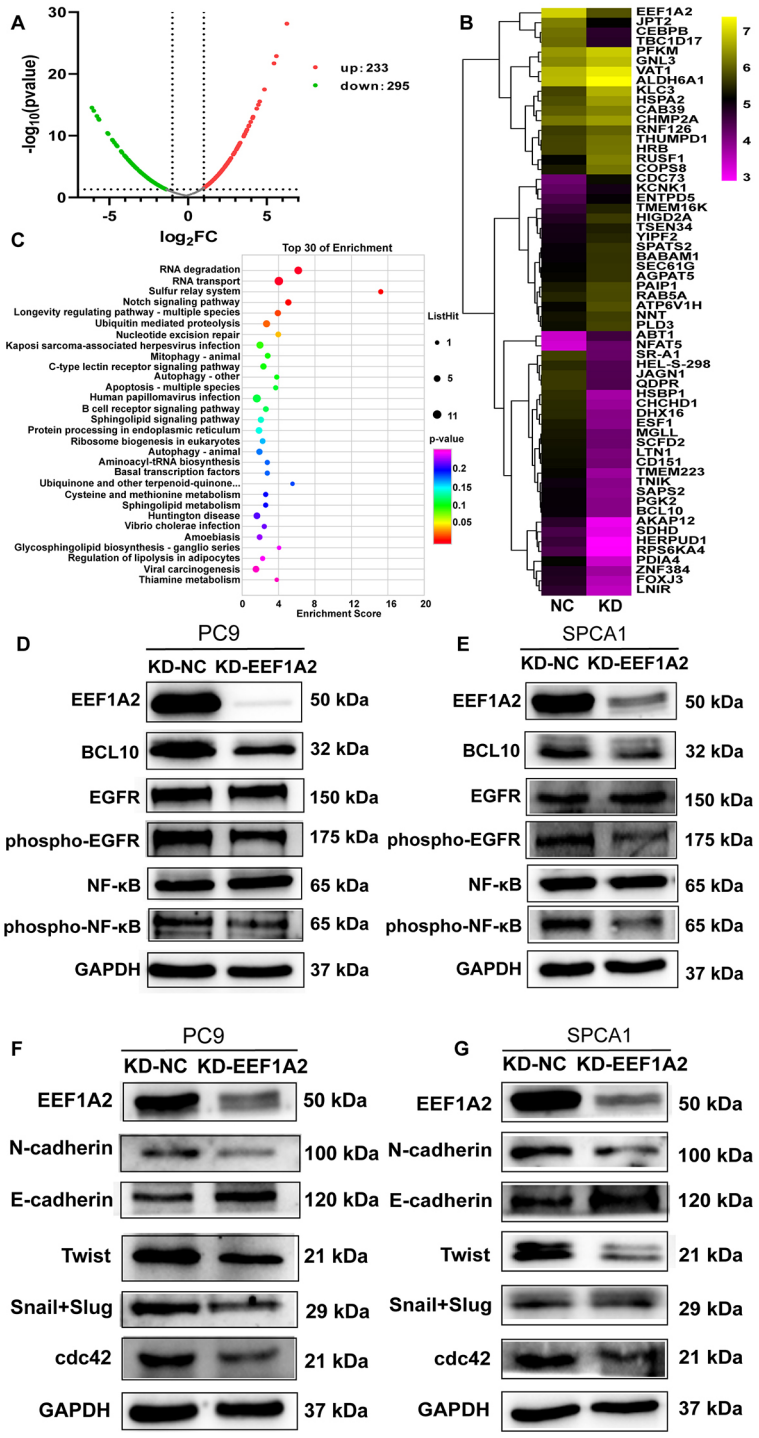

Figure 4. Knockdown of EEF1A2 reduces the expression of BCL10, NFκB and EMT-related molecules. (A) Volcano plots showing differentially expressed proteins (DEPs) in EEF1A2-knockdown PC9 cells. (B) Heatmaps demonstrating the top 30 up- and downregulated proteins. (C) KEGG analysis revealing the functional enrichment of 528 DEPs. (D-G) Western blot analysis of EEF1A2, BCL10, EGFR, phosphorylated EGFR (phospho-EGFR), NFκB, phosphorylated NFκB (phospho-NFκB), N-cadherin, E-cadherin, Twist, Snail + Slug, and Cdc42 in EEF1A2-knockdown PC9 and SPCA1 cells.

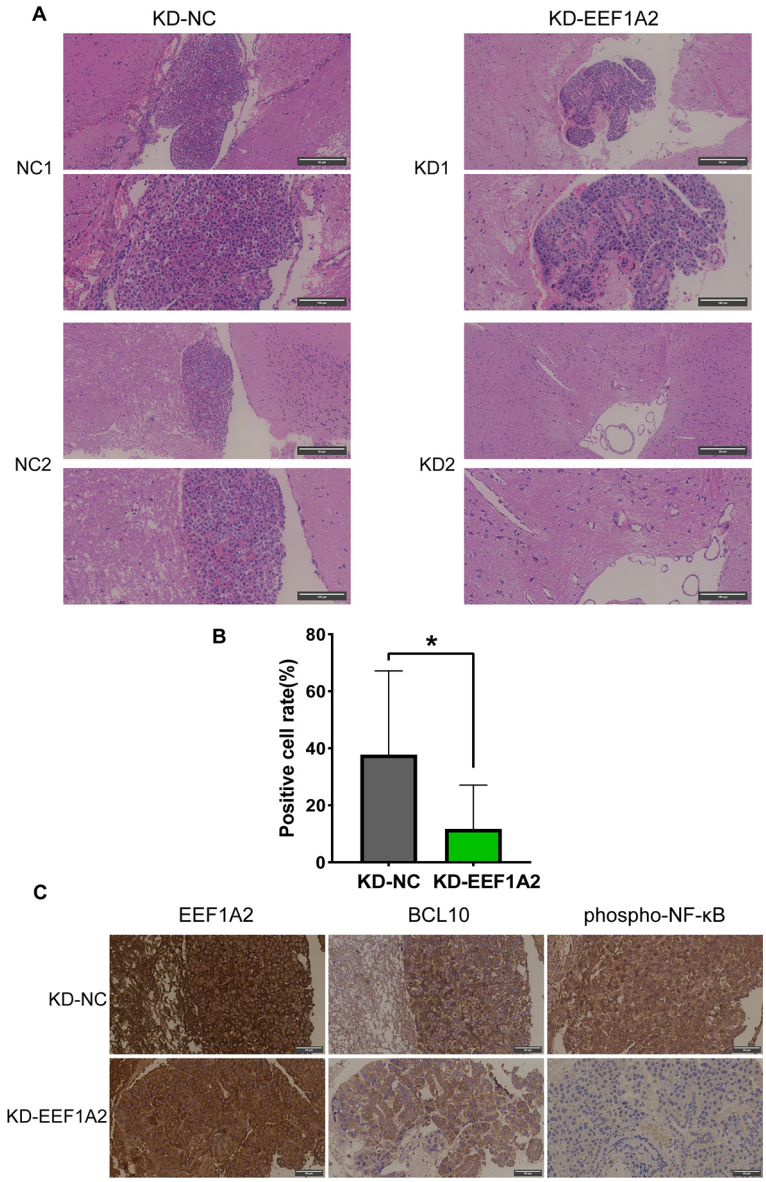

Figure 5. Knockdown of EEF1A2 inhibits lung cancer brain metastasis *in vivo*. (A) H&E staining of tumor tissue sections from brain metastases in nude mice. (B) Quantification of lung cancer cells in mouse brain tissues via H&E staining. **P* < 0.05. (C) IHC staining of EEF1A2, BCL10, and phosphorylated NFκB in mouse brain metastases.

demonstrated that EEF1A2 knockdown reduced the development of LCBM in nude mice. We have found that EEF1A2 enhances the metastasis of lung cancer cells to the brain by activating the BCL10/NFκB/EMT signaling pathway, leading to their aggressive behavior. This suggests that EEF1A2 could be a promising therapeutic target for developing more effective treatments for LCBM.

Comparative microarray analyses between LCBM and primary lung cancer revealed significant overexpression of metabolic processes, notably fructose metabolism, canonical glycolysis, and cellular amino acid biosynthesis, in brain metastases. Consuming about 20% of the body's energy derived from glucose, the brain displays metabolic flexibility to avoid energy shortages by utilizing a variety of nutrients. Brain metastases demonstrate metabolic adaptability through the use of glutamine and branched-chain

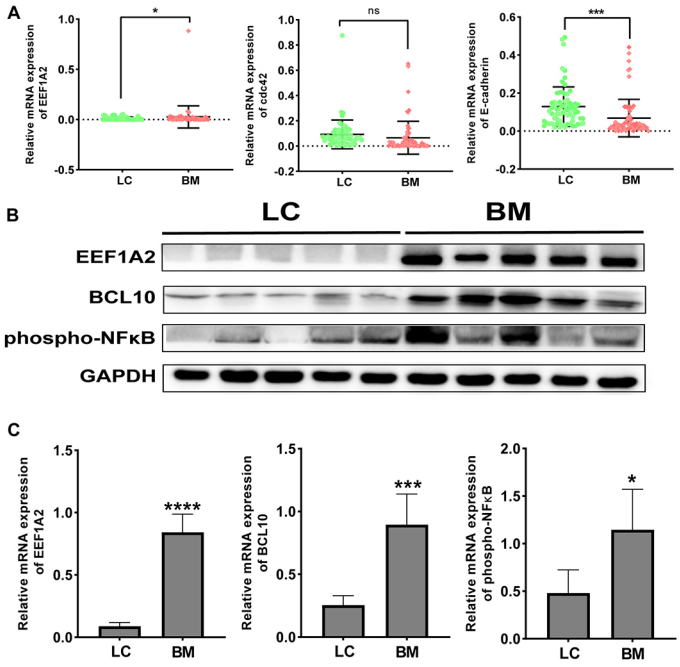

Figure 6. Increased expression of EEF1A2, BCL10 and phosphorylated NFκB in the LCBM. (A) RT-qPCR was used to determine the relative expression levels of EEF1A2, Cdc42, and E-cadherin genes in samples from 21 patients with LCBM and 21 patients with LC. *P < 0.05; ***P < 0.001; ns indicates no significant difference compared to the LC group. (B and C) Western blot analysis of EEF1A2, BCL10, and phosphorylated NFκB (phospho-NFκB) in tumor samples from five LC patients and five LCBM patients. *P < 0.05; ***P < 0.001; **** P < 0.0001.

amino acids as alternative energy sources[17,18]; for example, phosphoglycerate dehydrogenase (PHGDH) promotes brain metastasis progression via increased serine synthesis[19,20]. Brain metastases exhibit metabolic flexibility by using glutamine and branched-chain amino acids as alternative energy sources[17,18]. For instance, phosphoglycerate dehydrogenase (PHGDH) promotes the progression of brain metastases by increasing serine synthesis[19,20]. Conversely, genes downregulated in the LCBM are associated mainly with "cell adhesion" and "focal adhesion". Alterations in the adhesive properties of neoplastic cells are critical in cancer development and progression[21,22]; loss of intercellular adhesion and detachment from the lamina propria facilitate malignant cell escape, extracellular matrix degradation, acquisition of motility and invasiveness, and eventual metastasis[23,24]. Targeted therapies against intercellular adhesion molecules have been extensively explored for the treatment of cancer metastasis[25,26]. In lung cancer, the downregulation of adhesion-related molecules, combined with increased carbohydrate and amino acid metabolism, appears to increase the metastatic potential.

EEF1A2 is a significant oncogene implicated in multiple malignancies, including cancers of the breast, liver, stomach, pancreas, and lungs[27-29]. Its overexpression is typically associated with poor prognosis in pancreatic cancer, NSCLC, and ovarian cancer[30,31]. As prognosis is closely linked to metastasis, especially distant metastases such as lung and brain metastases, uncovering the impact of EEF1A2 in tumor metastasis is pivotal for improving treatment outcomes. Previous studies have shown that EEF1A2 enhances EMT and promotes lung and lymph node metastasis in LUAD[32]; however, its impact on brain metastasis in patients with lung cancer remains unexplored. Our research demonstrated that EEF1A2 expression was significantly increased in LCBM, and that reducing EEF1A2 levels significantly hindered brain metastasis in nude mice. Research has explored the mechanisms by which EEF1A2 contributes to tumorigenesis. Initially, it was proposed that EEF1A2 might impact tumor development by regulating translation rates, similar to the role

of eukaryotic initiation factor 4E (EIF4E)[33]. However, recent studies have indicated that EEF1A2 interacts with F-actin, affects cytoskeletal remodeling[34,35], and regulates key signaling pathways controlling cell division, apoptosis, migration, and invasion, including the JAK/STAT, AKT, and PI3K/AKT/mTOR pathways[36,37]. These results indicate that EEF1A2 is a valuable target for preventing brain metastasis in lung cancer patients, offering potential paths for therapeutic intervention.

Despite EEF1A2 being recognized for activating the PI3K/AKT pathway and promoting tumor cell migration and invasion, our study did not observe this effect. Instead, proteomic analysis revealed a significant decrease in BCL10 expression upon EEF1A2 knockdown. BCL10 is involved in gastric mucosa-associated lymphoid tissue (MALT) lymphoma and is frequently linked to the chromosomal translocation t(1;14)(p22;q32)[38]. This translocation leads to the production of a protein that activates NFκB. Its expression has been reported in various malignancies, including cancers of the stomach, breast, liver, colon, rectum, and pancreas[39-41]. BCL10 is engaged in a variety of signaling pathways, including those regulated by G protein-coupled, epidermal growth factor, and vascular endothelial growth factor receptors, contributing to cancer progression[42-44]. Specifically, BCL10 contributes to the activation of NFκB transcription factors[45]. Our study revealed elevated levels of both BCL10 and phosphorylated NFκB in the LCBM. Notably, EEF1A2 depletion led to a simultaneous reduction in BCL10 and phosphorylated NFκB levels. These findings implicate EEF1A2 as a potential key player in the BCL10/NFκB pathway, suggesting its critical involvement in the pathogenesis of LCBM.

NFκB signaling, widely acknowledged for its tumor-promoting properties, facilitates metastatic dissemination by driving the EMT, a phenomenon linked to multiple malignancies, including those of the brain, breast, lung, and stomach[46]. EMT is a fundamental process that drives changes in cellular morphology and plays a crucial role in tumor progression, particularly during the metastasis, spread, and colonization of cancer cells[47,48]. During EMT, epithelial cells transition from a polarized, stationary state to a nonpolarized, motile, and invasive phenotype. This transition is regulated by EMT-specific transcription factors such as ZEB1/2, SNAIL, and SLUG[49,50]. Our research demonstrated that the knockdown of EEF1A2 disrupted the EMT machinery. Specifically, we observed the upregulation of E-cadherin and the downregulation of N-cadherin, Twist, Cdc42, Snail, and Slug. These alterations suggest that EEF1A2 contributes to the formation of the LCBM by facilitating EMT. By allowing cancer cells to detach from the primary tumor, invade neighboring stromal tissue, and enter the circulatory system, this transition supports the initial stages of metastasis. However, metastasis is a complex, multistep process that extends beyond EMT. This process includes not only the invasion of local areas but also the entry of cancer cells into the bloodstream or lymphatic vessels (intravasation), their survival during circulation, extravasation into distant tissues, and the formation of secondary tumors through colonization. Therefore, while EMT contributes to the increased invasive and migratory potential of cancer cells, it is distinct from the full metastatic cascade. In our study, the observed alterations in EMT-related protein expression following EEF1A2 knockdown indicate a reversal of the EMT process, which may reduce the cells' invasive capabilities and potential for initiating metastasis.

CONCLUSION

Our research reveals that EEF1A2 is instrumental in the tumor formation, progression, migration, and spread of lung cancer cells through the BCL10/NFκB pathway. Moreover, we demonstrate that silencing EEF1A2 significantly inhibited LCBM, suggesting that EEF1A2 could be a promising therapeutic target for treating LCBM.

DECLARATIONS

Acknowledgments

The authors extend sincerest thanks to the patients who participated in the study to provide clinical samples. The authors are grateful to the Open and Shared Science and Technology Service Platform at Yunnan University of Chinese Medicine.

Authors' contributions

Study design: Wang J, Fan Y, Su X
Data analysis and interpretation: Li B, Zhou J, Ding K, Zeng B, Li S, Zhang L
Collection of samples: Yuan H, Zuo P
Data collection and assembly: Wang C, Liu S
Writing, discussion, revision, and improvement of the manuscript: Su X, Li B
All the authors have read and approved the final manuscript.

Availability of data and materials

The data reported in this paper have been deposited in OMIX, China National Center for Bioinformation/Beijing Institute of Genomics, Chinese Academy of Sciences (https://ngdc.cncb.ac.cn/omix/release/OMIX004271 and https://ngdc.cncb.ac.cn/omix/release/OMIX004272).

Financial support and sponsorship

This study was supported by the National Nature Science Foundation of China (NSFC, 81960455, 82060519, 81760519 and 81960215), Yunnan Provincial Science and Technology Department, Kunming Medical University Joint Special Project for Applied Basic Research (202001AY070001-080), and Yunnan Provincial Department of Education Scientific Research Fund Project (2019J1274).

Conflicts of interest

All authors declared that there are no conflicts of interest.

Ethical approval and consent to participate

This research complied with the Declaration of Helsinki and was approved by the Ethics Committee of the Third Affiliated Hospital of Kunming Medical University (KY2019065). Informed consent was secured from all participants before collecting and utilizing their biological samples.

Consent for publication

Written informed consent was obtained from the patient for publication.

REFERENCES

1. Sung H, Ferlay J, Siegel RL, et al. Global cancer statistics 2020: GLOBOCAN estimates of incidence and mortality worldwide for 36 cancers in 185 countries. *CA Cancer J Clin.* 2021;71:209-49. DOI
2. Lamba N, Wen PY, Aizer AA. Epidemiology of brain metastases and leptomeningeal disease. *Neuro Oncol.* 2021;23:1447-56. DOI PubMed PMC
3. Vogelbaum MA, Brown PD, Messersmith H, et al. Treatment for brain metastases: ASCO-SNO-ASTRO guideline. *J Clin Oncol.* 2022;40:492-516. DOI
4. Negrutskii BS, El'skaya AV. Eukaryotic translation elongation factor 1α: structure, expression, functions, and possible role in aminoacyl-tRNA channeling. In: Progress in Nucleic Acid Research and Molecular Biology. Elsevier; 1998. pp. 47-78. DOI
5. Dever TE, Dinman JD, Green R. Translation elongation and recoding in eukaryotes. *Cold Spring Harb Perspect Biol.* 2018;10:a032649. DOI PubMed PMC

6. Anand N, Murthy S, Amann G, et al. Protein elongation factor EEF1A2 is a putative oncogene in ovarian cancer. *Nat Genet.* 2002;31:301-5. DOI
7. Pinke DE, Kalloger SE, Francetic T, Huntsman DG, Lee JM. The prognostic significance of elongation factor eEF1A2 in ovarian cancer. *Gynecol Oncol.* 2008;108:561-8. DOI PubMed
8. Tomlinson VA, Newbery HJ, Wray NR, et al. Translation elongation factor eEF1A2 is a potential oncoprotein that is overexpressed in two-thirds of breast tumours. *BMC Cancer.* 2005;5:113. DOI PubMed PMC
9. Lam DC, Girard L, Suen W, et al. Establishment and expression profiling of new lung cancer cell lines from chinese smokers and lifetime never-smokers. *J Thorac Oncol.* 2006;1:932-42. DOI
10. Schlaeger C, Longerich T, Schiller C, et al. Etiology-dependent molecular mechanisms in human hepatocarcinogenesis. *Hepatology.* 2008;47:511-20. DOI
11. Amiri A, Noei F, Jeganathan S, Kulkarni G, Pinke DE, Lee JM. eEF1A2 activates Akt and stimulates Akt-dependent actin remodeling, invasion and migration. *Oncogene.* 2007;26:3027-40. DOI PubMed
12. Xu C, Hu DM, Zhu Q. eEF1A2 promotes cell migration, invasion and metastasis in pancreatic cancer by upregulating MMP-9 expression through Akt activation. *Clin Exp Metastasis.* 2013;30:933-44. DOI PubMed
13. Giudici F, Petracci E, Nanni O, et al. Elevated levels of eEF1A2 protein expression in triple negative breast cancer relate with poor prognosis. *PLoS One.* 2019;14:e0218030. DOI PubMed PMC
14. Qiu FN, Huang Y, Chen DY, et al. Eukaryotic elongation factor-1α 2 knockdown inhibits hepatocarcinogenesis by suppressing PI3K/Akt/NF-κB signaling. *World J Gastroenterol.* 2016;22:4226-37. DOI PubMed PMC
15. Biswas DK, Iglehart JD. Linkage between EGFR family receptors and nuclear factor kappaB (NF-kappaB) signaling in breast cancer. *J Cell Physiol.* 2006;209:645-52. DOI PubMed
16. Achrol AS, Rennert RC, Anders C, et al. Brain metastases. *Nat Rev Dis Primers.* 2019;5:5. DOI
17. Bhutia YD, Ganapathy V. Glutamine transporters in mammalian cells and their functions in physiology and cancer. *Biochim Biophys Acta.* 2016;1863:2531-9. DOI PubMed PMC
18. Zhang B, Chen Y, Shi X, et al. Regulation of branched-chain amino acid metabolism by hypoxia-inducible factor in glioblastoma. *Cell Mol Life Sci.* 2021;78:195-206. DOI PubMed PMC
19. Ngo B, Kim E, Osorio-Vasquez V, et al. Limited environmental serine and glycine confer brain metastasis sensitivity to PHGDH inhibition. *Cancer Discov.* 2020;10:1352-73. DOI PubMed PMC
20. Liu J, Guo S, Li Q, et al. Phosphoglycerate dehydrogenase induces glioma cells proliferation and invasion by stabilizing forkhead box M1. *J Neurooncol.* 2013;111:245-55. DOI PubMed PMC
21. Horzum U, Ozdil B, Pesen-Okvur D. Differentiation of normal and cancer cell adhesion on custom designed protein nanopatterns. *Nano Lett.* 2015;15:5393-403. DOI PubMed
22. Tilghman RW, Parsons JT. Focal adhesion kinase as a regulator of cell tension in the progression of cancer. *Semin Cancer Biol.* 2008;18:45-52. DOI PubMed PMC
23. Lauko A, Mu Z, Gutmann DH, Naik UP, Lathia JD. Junctional adhesion molecules in cancer: a paradigm for the diverse functions of cell-cell interactions in tumor progression. *Cancer Res.* 2020;80:4878-85. DOI PubMed PMC
24. Hirohashi S, Kanai Y. Cell adhesion system and human cancer morphogenesis. *Cancer Sci.* 2003;94:575-81. DOI PubMed PMC
25. Lafrenie RM, Buckner CA, Bewick MA. Cell adhesion and cancer: is there a potential for therapeutic intervention? *Expert Opin Ther Targets.* 2007;11:727-31. DOI
26. Eke I, Cordes N. Focal adhesion signaling and therapy resistance in cancer. *Semin Cancer Biol.* 2015;31:65-75. DOI PubMed
27. Patel SA, Hassan MK, Naik M, et al. EEF1A2 promotes HIF1A mediated breast cancer angiogenesis in normoxia and participates in a positive feedback loop with HIF1A in hypoxia. *Br J Cancer.* 2024;130:184-200. DOI PubMed PMC
28. Yang S, Lu M, Chen Y, et al. Overexpression of eukaryotic elongation factor 1 alpha-2 is associated with poorer prognosis in patients with gastric cancer. *J Cancer Res Clin Oncol.* 2015;141:1265-75. DOI
29. Patel SA, Hassan MK, Dixit M. Oncogenic activation of EEF1A2 expression: a journey from a putative to an established oncogene. *Cell Mol Biol Lett.* 2024;29:6. DOI PubMed PMC
30. Duanmin H, Chao X, Qi Z. eEF1A2 protein expression correlates with lymph node metastasis and decreased survival in pancreatic ductal adenocarcinoma. *Hepatogastroenterology.* 2013;60:870-5. DOI PubMed
31. Sun Y, Wong N, Guan Y, et al. The eukaryotic translation elongation factor eEF1A2 induces neoplastic properties and mediates tumorigenic effects of ZNF217 in precursor cells of human ovarian carcinomas. *Int J Cancer.* 2008;123:1761-9. DOI PubMed PMC
32. Jia L, Ge X, Du C, et al. EEF1A2 interacts with HSP90AB1 to promote lung adenocarcinoma metastasis via enhancing TGF-β/SMAD signalling. *Br J Cancer.* 2021;124:1301-11. DOI PubMed PMC
33. Thornton S, Anand N, Purcell D, Lee J. Not just for housekeeping: protein initiation and elongation factors in cell growth and tumorigenesis. *J Mol Med.* 2003;81:536-48. DOI PubMed
34. Mendoza MB, Gutierrez S, Ortiz R, et al. The elongation factor eEF1A2 controls translation and actin dynamics in dendritic spines. *Sci Signal.* 2021;14:eabf5594. DOI
35. Bodman JAR, Yang Y, Logan MR, Eitzen G. Yeast translation elongation factor-1A binds vacuole-localized Rho1p to facilitate membrane integrity through F-actin remodeling. *J Biol Chem.* 2015;290:4705-16. DOI PubMed PMC
36. Li Z, Qi CF, Shin DM, et al. Eef1a2 promotes cell growth, inhibits apoptosis and activates JAK/STAT and AKT signaling in mouse plasmacytomas. *PLoS One.* 2010;5:e10755. DOI PubMed PMC

37. Pellegrino R, Calvisi DF, Neumann O, et al. EEF1A2 inactivates p53 by way of PI3K/AKT/mTOR-dependent stabilization of MDM4 in hepatocellular carcinoma. *Hepatology.* 2014;59:1886-99. DOI PubMed PMC
38. Willis TG, Jadayel DM, Du MQ, et al. Bcl10 is involved in t(1;14)(p22;q32) of MALT B cell lymphoma and mutated in multiple tumor types. *Cell.* 1999;96:35-45. DOI
39. Ekambaram P, Lee JL, Hubel NE, et al. The CARMA3-Bcl10-MALT1 signalosome drives NFκB activation and promotes aggressiveness in angiotensin II receptor-positive breast cancer. *Cancer Res.* 2018;78:1225-40. DOI PubMed PMC
40. Holzmann K, Kohlhammer H, Schwaenen C, et al. Genomic DNA-chip hybridization reveals a higher incidence of genomic amplifications in pancreatic cancer than conventional comparative genomic hybridization and leads to the identification of novel candidate genes. *Cancer Res.* 2004;64:4428-33. DOI
41. Yeh PY, Kuo SH, Yeh KH, et al. A pathway for tumor necrosis factor-alpha-induced Bcl10 nuclear translocation. Bcl10 is up-regulated by NF-kappaB and phosphorylated by Akt1 and then complexes with Bcl3 to enter the nucleus. *J Biol Chem.* 2006;281:167-75. DOI PubMed
42. Wang D, You Y, Lin PC, et al. Bcl10 plays a critical role in NF-kappaB activation induced by G protein-coupled receptors. *Proc Natl Acad Sci USA.* 2007;104:145-50. DOI
43. Jiang T, Grabiner B, Zhu Y, et al. CARMA3 is crucial for EGFR-Induced activation of NF-κB and tumor progression. *Cancer Res.* 2011;71:2183-92. DOI PubMed PMC
44. Martin D, Galisteo R, Gutkind JS. CXCL8/IL8 stimulates vascular endothelial growth factor (VEGF) expression and the autocrine activation of VEGFR2 in endothelial cells by activating NFkappaB through the CBM (Carma3/Bcl10/Malt1) complex. *J Biol Chem.* 2009;284:6038-42. DOI PubMed PMC
45. Staudt LM. Oncogenic activation of NF-κB. *Cold Spring Harb Perspect Biol.* 2010;2:a000109. DOI PubMed PMC
46. Mirzaei S, Saghari S, Bassiri F, et al. NF-κB as a regulator of cancer metastasis and therapy response: a focus on epithelial-mesenchymal transition. *J Cell Physiol.* 2022;237:2770-95. DOI
47. Thiery JP, Sleeman JP. Complex networks orchestrate epithelial-mesenchymal transitions. *Nat Rev Mol Cell Biol.* 2006;7:131-42. DOI PubMed
48. Grünert S, Jechlinger M, Beug H. Diverse cellular and molecular mechanisms contribute to epithelial plasticity and metastasis. *Nat Rev Mol Cell Biol.* 2003;4:657-65. DOI PubMed
49. Yilmaz M, Christofori G. EMT, the cytoskeleton, and cancer cell invasion. *Cancer Metastasis Rev.* 2009;28:15-33. DOI PubMed
50. Yang S, Liu Y, Li MY, et al. FOXP3 promotes tumor growth and metastasis by activating Wnt/β-catenin signaling pathway and EMT in non-small cell lung cancer. *Mol Cancer.* 2017;16:124. DOI PubMed PMC